Variability and Invariability in the Structure of an Identified Nonspiking Interneuron of Crayfish as Revealed by Three-Dimensional Morphometry

Authors: Hikosaka, Ryou, Takahashi, Mikio, and Takahata, Masakazu

Source: Zoological Science, 13(1) : 69-78

Published By: Zoological Society of Japan

URL: https://doi.org/10.2108/zsj.13.69

ZOOLOGICAL SCIENCE 13: 69–78 (1996)

Variability and Invariability in the Structure of an Identified Nonspiking Interneuron of Crayfish as Revealed by Three-Dimensional Morphometry

Ryou Hikosaka, Mikio Takahashi and Masakazu Takahata

Division of Biological Sciences, Graduate School of Science, Hokkaido University, Sapporo 060, Japan

ABSTRACT—We have quantitatively analyzed the three-dimensional dendritic structure of an identified nonspiking interneuron, Local Directionally Selective (LDS) interneuron in the terminal abdominal ganglion of the crayfish, *Procambarus clarkii* Girard, using a confocal laser scanning microscopic system. Comparison of the cell size before and after fixation followed by dehydration and clearing revealed that the diameter of dendritic branches shrank by about 15% while the branch length showed no significant change. The soma and dendritic diameter in vivo were obtained from the measurement in the cleared preparation multiplied by the shrinkage factor.

The total length of dendrites and their membrane area as well as their electrotonic structure were found to vary from preparation to preparation. The spatial distribution of fine dendritic branches was variable, but that of major branches was constant among preparations. The interneuron further shared bilaterally asymmetrical dendritic structure: those branches on the soma side commonly showed larger membrane area and larger number of branching than those on the opposite side. The results indicate that the functional difference in the synaptic activity so far reported between dendrites on the soma side and those on the opposite side is paralleled by their differences in the dendritic morphology and electrotonic structure.

INTRODUCTION

Many nerve cells in the central nervous system of invertebrates are individually identifiable according to their physiological and morphological characteristics (Hoyle, 1975). Nonspiking interneurons, however, which have been reported to be present in the central nervous system of a variety of invertebrates (e.g. Burrows, 1976; Heitler *et al.*, 1980; Pearson *et al.*, 1975; Spencer, 1988; Takahata *et al.*, 1981), are not identifiable in general: cells with a similar pattern of dendritic branching and soma location form a cluster so that they can not be recognized individually (Goodman, 1978; Hisada *et al.*, 1984). One exception is the LDS (Local Directionally Selective) interneuron which is located in the terminal abdominal ganglion of the crayfish *Procambarus clarkii* and involved in the tailfan mechanosensory system (Krenz *et al.*, 1985; Reichert *et al.*, 1982; Reichert *et al.*, 1983). It has been reported that this cell can be individually identified by their structure and physiological properties including voltage-dependent inward and outward rectification (Takahashi *et al.*, 1995; Takahata *et al.*, 1995).

The LDS interneuron in every animal shares a common basic structure, having a single transverse segment crossing the midline and 2 major branches directly bifurcating from the transverse segment on both side. The interneuron can be repeatedly recognized from animal to animal according to this common basic structure, but, we reported in the previous papers that it showed a certain degree of morphological variability (Takahashi *et al.*, 1995; also see Reichert *et al.*, 1983). It has been long known in the central nervous system of invertebrates that the identified cells show morphological variability regarding their axonal and dendritic branching patterns (Burrows, 1973; Goodman, 1978; Macagno *et al.*, 1973; O'Shea *et al.*, 1974; Pearson *et al.*, 1979; Pearson *et al.*, 1980; Stretton *et al.*, 1973; Treistman *et al.*, 1976; Tweedle *et al.*, 1973). However, the structural analyses in these cells including the LDS interneuron have so far been based mostly on the comparison of camera lucida drawings of the projected image of these cells and therefore remained qualitative.

The dendrites of central neurons function in not only collecting synaptic inputs but also integrating them electrotonically based on their membrane properties and three-dimensional structure (Borst *et al.*, 1994; Rall *et al.*, 1992; Shepherd *et al.*, 1990). Since the output of the LDS interneuron is directly controlled by graded synaptic potentials instead of action potentials (Reichert *et al.*, 1983), its function depends on how the shape of synaptic potentials is transformed in the course of spread from the input to output synaptic regions. Quantitative analyses of the morphological variability in the dendritic structure of the LDS interneuron is therefore crucial for understanding its functional roles in mechanosensory information processing. In the present study, we quantitatively investigated the three-dimensional structure of the LDS interneuron by a confocal laser scanning microscopic system, which has been demonstrated to enable three-dimensional cell morphometry (Carlson *et al.*, 1989; Wallén *et al.*, 1988).

Accepted November 30, 1995
Received October 9, 1995

MATERIALS AND METHODS

Animals and preparation

Adult crayfish *Procambarus clarkii* Girard of both sexes, ranging from 8 to 10 cm in body length, were obtained commercially from a local dealer (Sankyo Labo, Sapporo). They were kept in laboratory tanks with running water until used in the experiment. The terminal (6th) abdominal ganglion was isolated from the rest of the body together with its ganglionic nerve roots. The ganglion was pinned down with the dorsal side up in a silicone-lined chamber which was filled with crayfish saline (Van Harreveld, 1936) at room temperature (20–25°C). The ganglionic sheath was left intact.

Electrophysiology and cell identification

Glass microelectrodes were filled with 3% Lucifer yellow dissolved in 1M LiCl. The electrode resistance was about 35 MΩ ranging 30–40 MΩ. The microelectrode was connected to a high input-impedance amplifier (Nihon-Kohden, CEZ-3100) whose output was sent to a storage oscilloscope (Tektronix 5113), a magnetic data recorder (TEAC, XR-50H) and a personal computer (NEC, PC-9801RX). Pin electrodes were placed in contact with the second and third ganglionic roots on both sides for their extracellular stimulation. They were coupled with an electronic stimulator through isolators. The impaled cell was first identified to be the LDS interneuron on the basis of physiological criteria (Takahata *et al.*, 1995) and finally confirmed by its morphology revealed by intracellular injection of a fluorescent dye Lucifer yellow CH (Stewart, 1978). For later analyses of the electrotonic structure of the cell, hyperpolarizing step current pulses were injected intracellularly through the recording microelectrode using the discrete current clamp method (Wilson *et al.*, 1975). The sampling frequency in the present study was 1.0–2.0 kHz. Transient responses of the cell to step current injection were used to extract the membrane time constant (Takahashi *et al.*, 1995). The interneuron was always impaled in the thick transverse segment on or near the midline. Methodological details on the physiological experiments are provided elsewhere (Takahata *et al.*, 1995).

After the physiological experiment was finished, the dye was iontophoretically injected into the cell by applying hyperpolarizing current pulses (5 –10 nA, 500 msec in duration, 1 Hz in frequency) for 15–30 min. The site of electrode impalement into the cell was monitored in situ under the dissecting microscope by the epiillumination method (Takahashi *et al.*, 1995). The preparation was then fixed in 10 % formaldehyde for 6 minutes, dehydrated in an ascending series of ethanol (each 2 minutes in 70, 95, 100%) and cleared in methyl salicylate. In some experiments, the preparation was examined before fixation under a confocal laser scanning microscope for measuring the diameter and length of dendritic branches *in vivo*. The results were compared with those obtained from the same preparation after fixation to estimate the shrinkage factor due to the clearing process.

Three-dimensional morphometry

In the morphological analysis 13 LDS interneurons were successfully stained. Each cell was optically sectioned using a confocal laser scanning microscope system (Sarastro 2000, Molecular Dynamics) including an Argon-ion laser, a Nikon Optiphoto II epifluorescence microscope and a Silicon Graphics Iris Indigo XS24 workstation. The preparation was always set with the dorsal side up on the microscope stage so that the X- and Y-axis in the three-dimensional coordinate system correspond respectively to the transverse and longitudinal axis of the animal body. The laser line of 457 nm in wavelength was selected from the Argon laser generator (25 mW power) having 3 lines (457, 488, 514 nm). The laser beam was focused to a point by a microscope lens and scanned the specimen with the aid of a two-mirror system driven by a galvanometric (Y-axis) and a stepping motor (X-axis). The fluorescent light from the specimen passed back through the microscope objective lens, dichroic beamsplitter mirror and achromat lens to the confocal pinhole aperture which was set to 50 μm to prevent out-of-focus light from reaching the photomultiplier detector. A long-pass barrier filter (510 nm) was placed behind the pinhole aperture.

With an objective lens of×10 (NA 0.45), each section was resolved into either 512×512 pixels with the size of 2×2 μm or 1024 ×1024 pixels of 1×1 μm in 256 gray scales. Scanning was repeated for 3-4 times at the same plane for averaging to improve the signal-to-noise ratio. The scanning plane was then changed by 1 or 2 μm in the Z-axis direction corresponding to the dorso-ventral axis of the animal body, using a stepping motor attached to the fine control of the microscope. Sectioning of the whole cell including the cell body and all dendritic branches resulted in a series of 147 to 267 sections with the stepsize of 2 μm. They were stored in a magneto-optical disk for later analyses.

The spatial distribution of individual dendritic branches was studied by examining the three-dimensional structure of the whole cell. We used a software (ImageSpace, version 3.0; Molecular Dynamics) implemented on the Sarastro 2000 system, to measure the diameter and length of each dendritic branch on the serial sections by re-displaying them on the workstation video screen. Each dendritic branch was represented by one cylinder or a connected sequence of cylinders each with specific diameter and length values. The whole LDS interneuron could be represented as an assembly of 418–645 cylinders. The length of each cylinder was calculated trigonometrically from the three-dimensional coordinates of the centers of its both ends. The diameter and length of dendrites in vivo were obtained by multiplying the measurements in the cleared specimen with the shrinkage factor (see above). The coordinates were stored together with diameters in a database running on a personal computer for quantitative presentation of the cell by a dendrogram (Fig.3). The dendrograms in this paper represent the real branch length, diameter and branching pattern of the interneuron in the three-dimensional space. The cell body was represented by an ellipsoid of revolution characterized by a revolution axis passing the attachment site of the dendrite with the cell body.

RESULTS

Cell shrinkage by clearing

Morphology of an LDS interneuron is compared as the horizontal projection image before and after the clearing process in Figure 1A, B. After fixation, dehydration and clearing, the interneuron apparently shrank to become smaller than before the clearing process. In order to examine the degree of the cell shrinkage, we have measured the length and diameter of major dendritic branches in 8 LDS interneurons from different preparations before and after the clearing process. Since the interneuron showed common basic branching pattern (see introduction), we selected 14 sites for the measurement of dendritic diameter and 4 sites for the measurement of length (Fig. 1C). The longest and shortest diameters of the soma were also examined. The diameter of dendritic branches and the soma were found to show significant shrinkage by the rate of 14.6±1.3 % (mean±SE) after clearing ($P< 0.01$ with Student's paired t-test). The length of dendritic branches decreased by 3.0±2.7% (Fig. 1D), but the difference was not statistically significant ($P> 0.05$). We found no significant difference in the shrinkage rate among different measurement sites and among different preparations ($P > 0.05$). It was thus suggested that the diameter of dendritic branches of the LDS interneuron shrank uniformly over the entire cell while the dendritic length remained unchanged. In

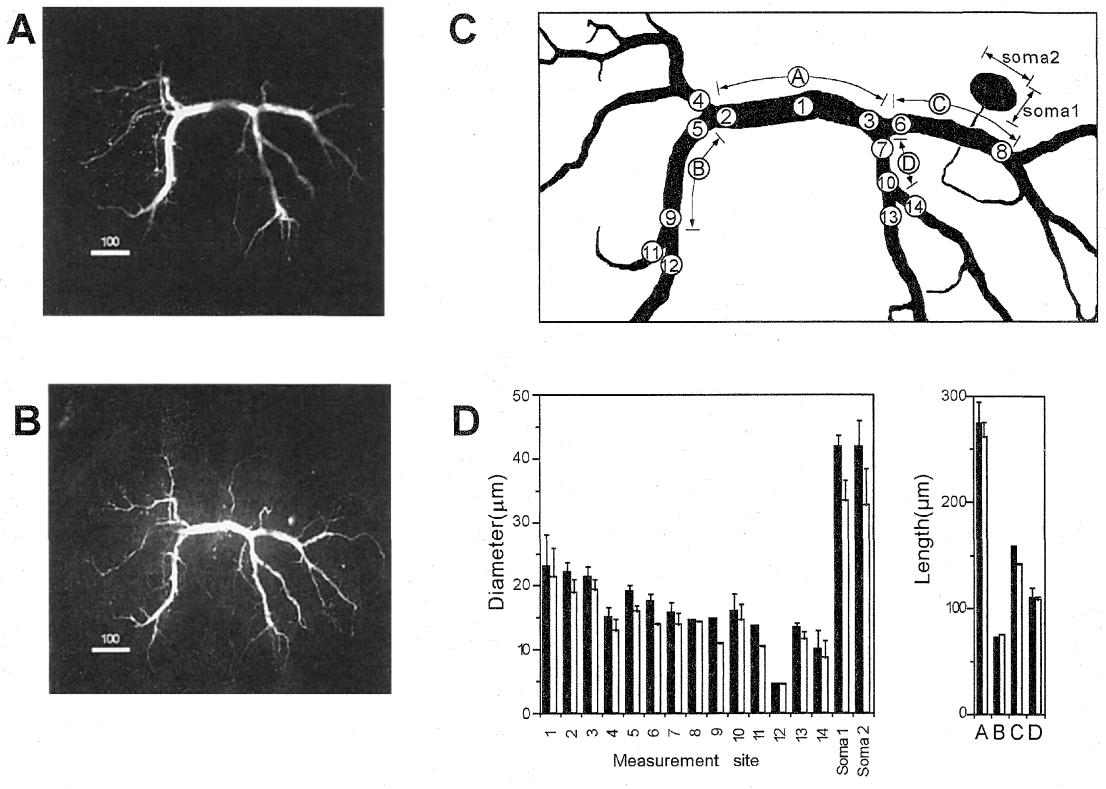

Fig. 1. Comparison of the LDS interneuron morphology before and after fixation followed by dehydration and clearing. A: Horizontal view before fixation. Horizontal optical sections of the cell made in a raw specimen were computationally projected on the same plane. B: Horizontal view after fixation. Calibration bar indicates 100 μm. C: Sites selected for measurement of shrinkage during clearing. 14 sites (1–14) for measurement of diameter and 4 sites (A-D) for measurement of length could be recognized in every preparation. The diameter of the cell body parallel to the revolution axis (soma1) and that perpendicular to it (soma2) were also measured. D: Results obtained from 8 preparations. Filled and open rectangles represent the mean values before and after fixation respectively. Bars represent standard errors of means.

the following part of this paper, the diameter of dendritic branches in vivo was determined by multiplying the measurements in the cleared preparation with the shrinkage factor of 1.17 (1/0.854).

Three-dimensional morphometry of the LDS interneuron

Projection images of an LDS interneuron are shown in Figure 2. The projection on the X-Y plane, i.e., the horizontal plane, was obtained by summing up all the optical sections with the stepsize of 2 μm (Fig. 2A1). The projection on the X-Z plane, i.e., the frontal plane (Fig. 2A2), and that on the Y-Z plane, i.e., the sagittal plane (Fig. 2A3), were obtained computationally by summing up the each profiles of optical sections with the interpolation function turned off. The cell was divided into numerous cylinders on the basis of the diameter and turning point of the dendrite. The diameter and length of each cylinder were measured in the three-dimensional coordinate system using the stack of optical sections. The cell structure was then reconstructed as an assembly of cylinders each of which representing the corresponding part of dendrites. The projection images of the reconstructed cell on the X-Y, X-Z and Y-Z planes are shown in Figure 2B1-3 respectively. The real diameter and length in vivo of each dendritic branch, together with the soma, are represented as the Sholl's dendrogram (Sholl, 1953) in Figure 2C. In this study, beaded swellings in the dendrites on the side opposite to the soma as observed by the silver-intensification method (Kondoh *et al.*, 1986) were not observed, although their size was reported to be large enough, ranging from 1.0 to 5.8 μm, for the spatial resolution of the confocal microscope. The dendrogram in the present study therefore does not include information on them.

Since the spread of synaptic current over the dendrite is dependent on the electrotonic structure of the cell (Rall, 1981; Rall *et al.*, 1992), we further calculated the electrotonic length of each branch by dividing the anatomical length by the space constant (λ) which was obtained from the relationship,

$$\lambda = \sqrt{\frac{D \cdot R_m}{4R_i}}$$

where D is the dendritic diameter, R_m the specific membrane resistance and R_i the specific resistance of cytoplasm. D was obtained from the current measurement, and R_i was assumed to be 60Ω·cm (Rall, 1977). R_m was obtained from the relationship, $t_m = R_m \cdot C_m$ where t_m is the membrane time constant as experimentally obtained in this study from the transient response of the cell to step current injection, and C_m, membrane capacitance per unit area, was assumed to be

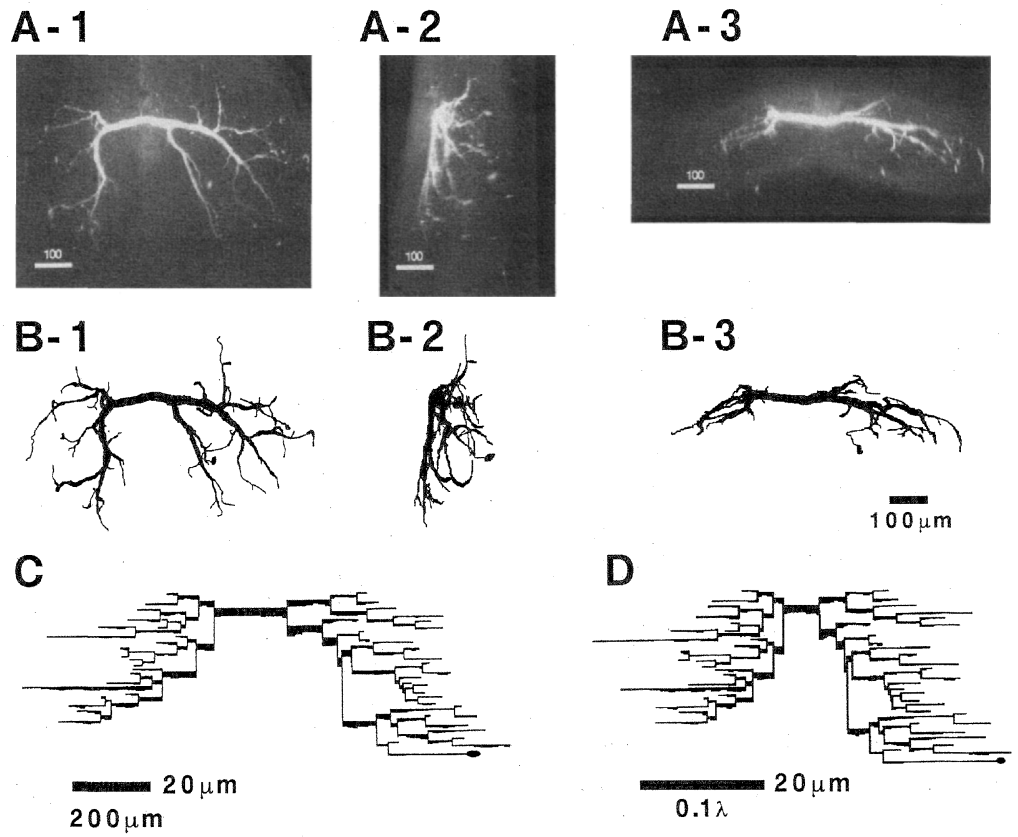

Fig. 2. Three dimensional morphometry of the LDS interneuron. A: Projected images of the cell on the horizontal (A-1), sagittal (A-2) and transverse (A-3) planes made computationally from horizontal optical sections of a fixed specimen. B: Projected images of the same cell represented by an assembly of 467 cylinders of different sizes on the horizontal (B-1), sagittal (B-2) and transverse (B-3) planes. Size of each cylinder is based on the three dimensional measurement conducted with the stack of optical sections. Each measurement was corrected by the shrinkage factor. The cell body is represented by an ellipsoid of revolution. C: Sholl's dendrogram of the same cell showing the anatomical length and diameter of individual branches. The cell body is represented by an ellipse with its long and short diameters indicating the real values. D: Dendrogram showing the electrotonic length of individual branches with their diameter. The cell body is regarded to be isopotential and therefore has no electrotonic length, but it is shown in this diagram with an ellipse to indicate its position.

1 μF/cm^2 (Rall, 1977). The electrotonic length of each branch is shown in Figure 2D. R_m was 12.4$\pm$1.3 kΩ·cm^2, ranging from 5.8 to 20.5.

Dendrograms of ten representative cells are illustrated in Figure 3. Comparison of dendritic structure based on these dendrograms showing anatomical and electrotonic properties of dendrites (Figs. 2C, D and 3) has revealed that individual interneuron differs from each other in several morphometrical parameters by a factor of 3.1 at the largest, including the total membrane area (ranging from 234,045 to 530,427 μm^2), the total dendritic length (5,645 to 12,978 μm), the length from the midline to the terminal of the longest dendritic branch (605 to 933 μm), the mean length from the midline to the terminal of all dendritic branches (378.8 to 536.7 μm), the number of branching (48 to 91), maximal electrotonic length from the midline to the dendritic terminal (0.17 to 0.42), and the mean electrotonic length from the midline to the terminal of all branches (0.10 to 0.22; Table 1).

Spatial distribution of dendrites in the neuropile

Superimposition of the three-dimensional structure of 13 LDS interneurons has revealed that the major branches (≥10 μm in diameter) of the interneuron show almost constant spatial distribution in the ganglionic neuropile in every preparation whereas the branching pattern of peripheral dendrites (<10 μm in diameter) show considerable variability from animal to animal (Fig. 4A-C). The position of each cell in the neuropile was normalized by assigning the transverse segment on the midline as the origin of the three-dimensional coordinate system. The neuropilar space was divided into 10 μm cubes and the number of intersection of each cube by the dendrite was counted for all 13 interneurons. The brighter part indicates that it is shared by larger number of interneurons. It is noted that the bright cubes make up a branching pattern common to individual cells especially on the X-Y plane (cf. Figs. 2A and 4A). On the Y-Z (Fig. 4B) and X-Z plane (Fig. 4C), although the bright regions are less demarcated than on the X-Y plane, the branching of major dendrites can be discriminated from the other parts of the cell. The dark part shown with an

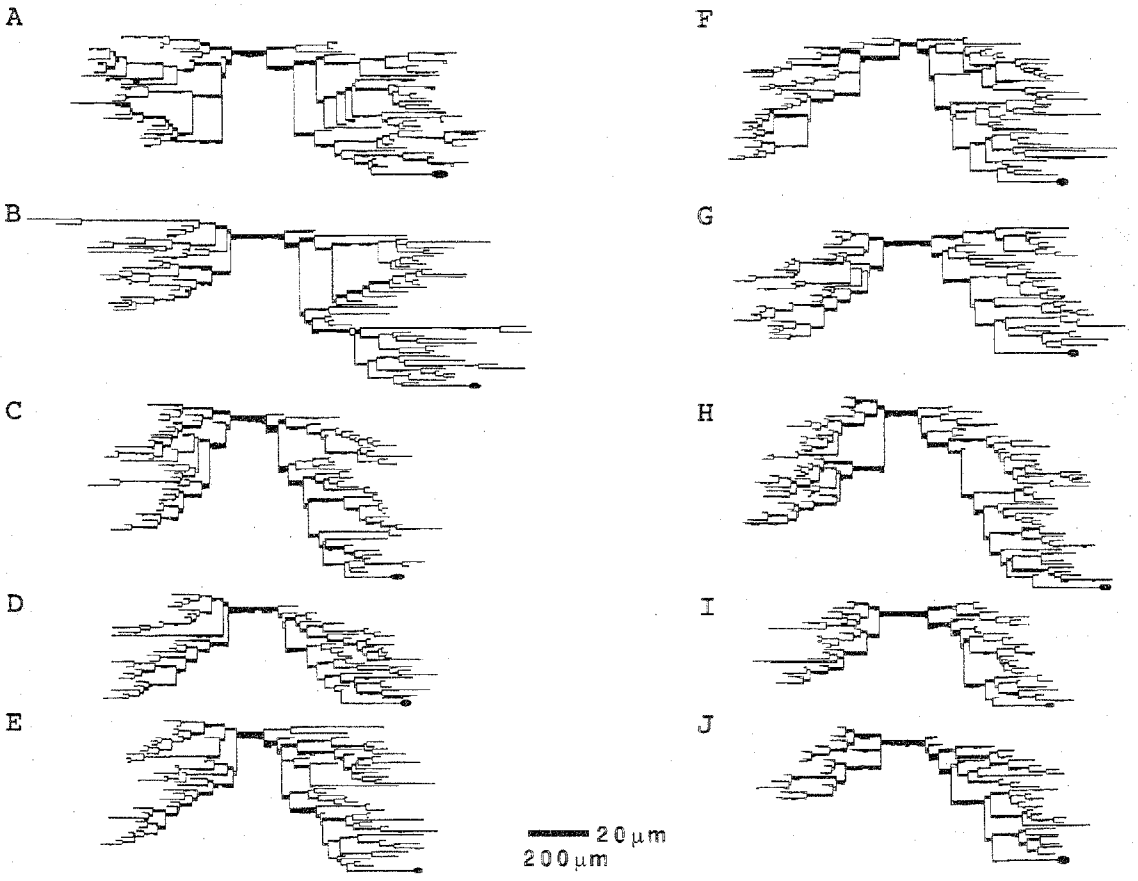

Fig. 3. Variation in the morphology of the LDS interneuron as revealed by its dendrograms from 10 different preparations, showing the anatomical length and diameter of individual branches.

Table 1. Morphometrical characteristics of the LDS interneuron*

	Both sides		Ipsilateral**		Contralateral**	
	Mean±SE	range	Mean±SE	range	Mean±SE	range
Total length						
Anatomical (μm)	9,384.5±598.5	5,645–12,978	5,962.4±395.6	3,229–8,381	3,425.2±231.4	1,888–4,597
Electrotonic (λ)	5.1±0.5	2.3–7.2	3.3±0.3	1.2–4.7	1.8±0.2	0.7–2.5
Total membrane area (μm^2)	346,794±20,913	234,045–530,427	203,443±12,550	133,422–304,057	143,851±9,173	103,263–226,370
Mean length from midline to terminal						
Anatomical (μm)	452.3±14.1	378.8–536.7	470.7±16.7	400.4–553.5	440.6±16.6	342.4–562.0
Electrotonic (λ)	0.16±0.01	0.10–0.22	0.18±0.01	0.10–0.25	0.15±0.01	0.09–0.20
Maximal length from midle to terminal						
Anatomical (μm)	744.2±29.7	605–933	743.9±29.8	604–933	633.9±31.7	401–897
Electrotonic (λ)	0.30±0.02	0.17–0.42	0.30±0.03	0.16–0.42	0.25±0.02	0.17–0.41
Mean number of branching	74±4	48–91	44±2	29–53	31±2	16–41

* Results obtained from 13 cells are summarized.
** Ipsilateral side refers to the side on which the soma is located. Contralateral side is the opposite side to the soma.

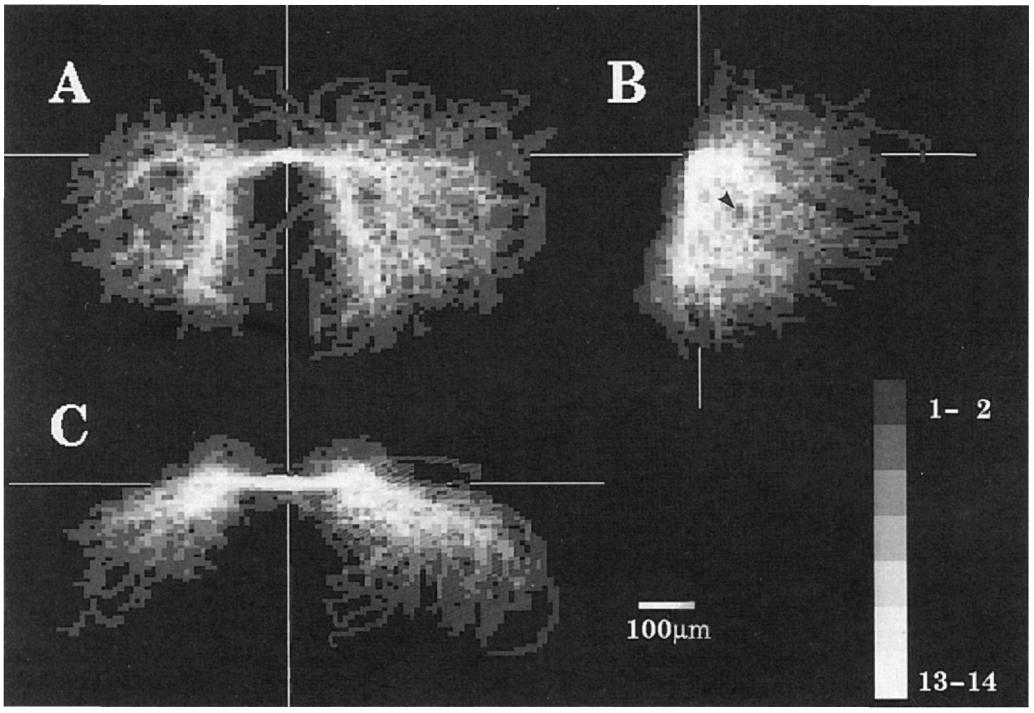

Fig. 4 . Three dimensional distribution of dendritic branches of the LDS interneuron in a coordinate system whose X, Y and Z axes correspond to the transverse, longitudinal and vertical axes of the animal body respectively. The origin of the coordinate axes was set to the crossing point of the transverse segment with the midline. The three dimensional neuropilar space was divided into 10 μm cubes starting from the coordinate origin. Number of intersection of each cube by dendritic branches was counted for all 13 interneurons. Brighter cubes indicate that they were intersected by larger number of cells than darker cubes. A: Horizontal view. B: Sagittal view. C: Transverse view.

arrowhead in Figure 4B apparently corresponds to the sensory commissure I in the sixth abdominal neuromere, an axon bundle of sensory neurons crossing the midline (A6SCI; Kondoh *et al.*, 1986). The position of the soma was also variable depending on the preparation.

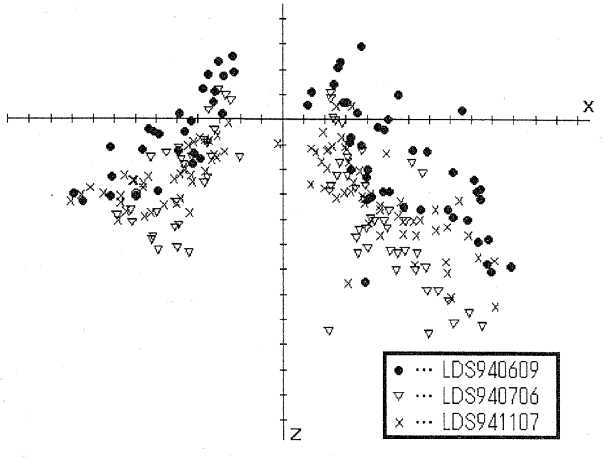

Fig. 5. Distribution of dendritic terminals in the transverse plane. Terminals of 3 representative cells are shown. They make clusters with partial overlapping and interdigitation, showing different pattern of spatial distribution.

Spatial distribution of the terminals of each dendritic branch was also found to differ from animal to animal. Dendritic terminals of three representative cells projected on the X-Z plane are illustrated in Figure 5. It is noted that each cell has clusters of terminals in different locations. Thus the three-dimensional morphometry has revealed that the same LDS interneuron shows variability in their dendritic structure in the individuals although it commonly shares basic branching pattern of major dendrites.

Common morphological characteristics of the LDS interneuron

Except the basic branching pattern of major dendrites, the LDS interneuron showed morphological variability. But quantitative comparison of the dendritic structure on the side ipsilateral to the soma with that on the opposite side revealed that the interneuron shared bilaterally asymmetrical dendritic structure in every preparation (Table 1; Fig. 6A). Dendrites on the soma side were significantly longer in the total anatomical length, and larger in the total area and in the number of branching than those on the opposite side ($P<0.01$). In particular, the length of dendrites whose diameter is less than 6 μm is significantly greater on the soma side than on the opposite side. There was no significant difference in the length of dendrites whose diameter was larger than 6 μm between both sides. Thus the difference in the total length of dendrites between the two sides is due to the difference in the length of

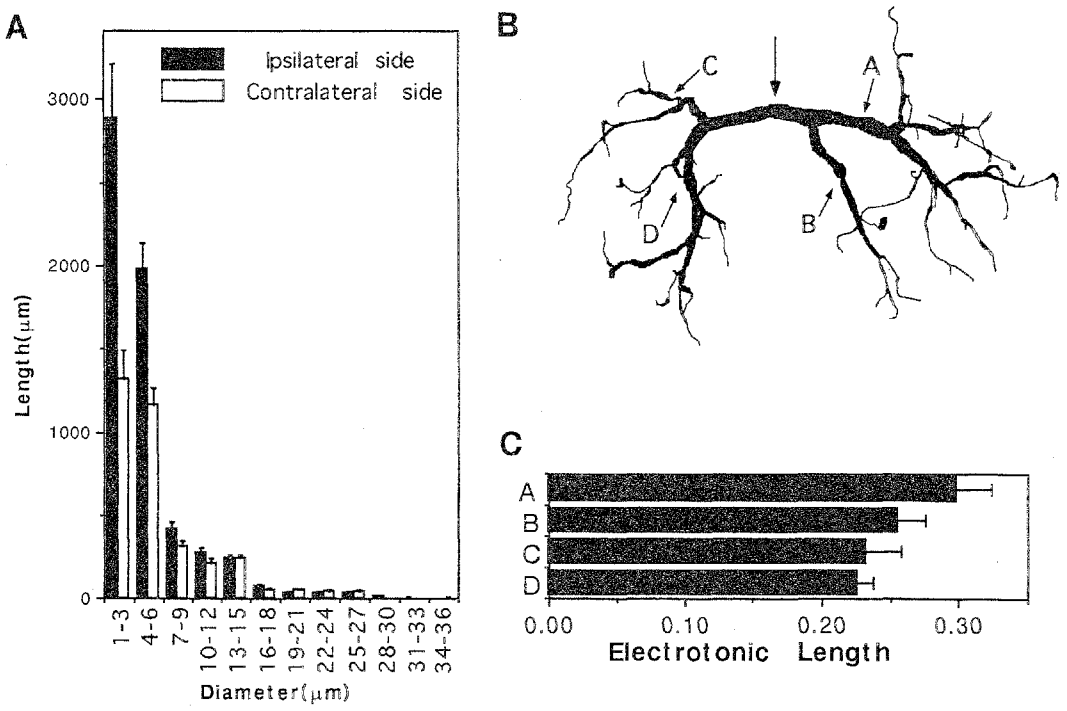

Fig. 6. Comparison of the dendritic structure between the side ipsilateral to the cell body and the opposite side. A: Histogram showing the total anatomical length of dendritic branches having different diameters. Filled and open rectangles indicate the mean value of measurement on the ipsilateral and contralateral side respectively. Bars represent standard errors of means. Dendrites having small diameters (<6 μm) was longer on the ipsilateral side than on the contralateral side ($P<0.01$). Thicker dendrites showed no difference in length between the two sides. B: 4 major branches (A-D) selected for comparison of the electrotonic length of dendritic branches. These branches could be discriminated in every preparation. C: Electrotonic length from the midline (shown with an arrow) to the most distant terminal of each branch. The differences between A and C, A and D, B and C, and B and D were statistically different ($P<0.01$). Results were obtained from the same 13 interneurons summarized in Table 1.

fine dendrites. The mean electrotonic length between the midline and the most distal dendritic termination of 2 representative major branches on the soma side was also significantly longer ($P<0.01$) than that of 2 major branches on the opposite side (Fig. 6B, C).

DISCUSSION

The confocal laser scanning fluorescence microscopy has been demonstrated to provide high-quality three-dimensional images of nerve cells (Brodin *et al.*, 1988; Carlson *et al.*, 1989; Mossberg *et al.*, 1990; Wallén *et al.*, 1988). With the conventional fluorescence microscopy, it is often difficult to quantitatively analyze the cell structure because of a 'halo' around strongly fluorescent elements and light scattering during traveling through the specimen (Cullheim *et al.*, 1987; Fleshman *et al.*, 1988; Ulfake *et al.*, 1981). In the confocal microscopy, the specimen is illuminated point-wise by a focused beam of light, and only the light emitted from the focal point is electronically detected (Wilson *et al.*, 1984). Consequently, the out-of-focus information is significantly suppressed to greatly improve image quality. Taking advantage of this confocal laser scanning microscopy, we have quantitatively investigated the dendritic structure of an identified nonspiking interneuron of crayfish and found that it varies from animal to animal while retaining the basic morphological pattern. We will discuss below the functional significance of variability and invariability in the dendritic structure of the interneuron.

Variability in the LDS interneuron morphology

Although morphological variability of the LDS interneuron has been qualitatively known (Reichert *et al.*, 1983; Takahashi *et al.*, 1995), we have quantitatively shown for the first time how the dendritic structure of the interneuron varies in individuals. It was revealed that the total dendritic length including branches on the soma side and those on the opposite side ranged from 234,045 to 530,427 μm^2 (N=13) (Table 1). Accordingly, the total membrane area varied among preparations. In addition to other anatomical characteristics, the mean electrotonic length from the midline to the terminal of all branches ranged from 0.10 to 0.22 (Table 1).

It should be noted here that the possibility that some branches in certain cases are not stained incidentally is unlikely from the following reasons: 1) the entire cell structure was stained brightly and the termination of individual branches was demarcated unambiguously from the background in each case, 2) the dye was always injected from the same part of

the cell, i.e., the thick transverse segment on the midline, and 3) the cell body which was connected to a major dendritic branch with a long thin process and was most difficult to be stained was always visible. We therefore conclude that the observed difference in the dendritic structure reflects its intrinsic variability rather than any artifactual capriciousness of intracellular staining.

Since the dendrites of the LDS interneuron, as those of other local nonspiking interneurons, function not only in receiving synaptic inputs but also in releasing transmitters for the postsynaptic cells, the variability in dendritic structure is likely to result in functional variability of the interneuron. In particular, the finding that the spatial distribution of fine dendrites (Fig. 4) and their termination sites (Fig. 5) are variable, although that of major branches is rather constant (Fig.4), is functionally relevant since an electronmicroscopic study has revealed that most synapses are distributed over fine dendrites and not at all over major ones (Kondoh *et al.*, 1986). If the spatial distribution of pre- and post-synaptic cell processes remains unchanged, the different branching pattern of fine dendrites of the LDS interneuron would lead to different synaptic connection of the interneuron with those cells. The fact that the mean electrotonic length from the midline to the terminal of all branches varies among preparations (Table 1) further indicates that the spatio-temporal distribution of synaptic potentials over dendrites is also variable although it is not determined solely by the electrotonic length of each branch but affected by the electrotonic structure of the whole cell (Jack, 1979; Rall, 1977, 1981; Rall *et al.*, 1992).

Although the synaptic response of the LDS interneuron has been reported to be variable among preparations (Krenz *et al.*, 1985; Reichert *et al.*, 1983; Takahata *et al.*, 1995), we can not at present relate this functional variability to any morphological one since the physiological experiment on the synaptic activity of the interneuron has so far been done in the condition that the sensory neurons that are presynaptic to the interneuron are stimulated not singularly but in concert (Krenz *et al.*, 1985; Nagayama *et al.*, 1988; Reichert *et al.*, 1982, 1983; Takahashi *et al.*, 1995; Takahata *et al.*, 1995). For understanding the function of dendritic structure in receiving synaptic inputs, synaptic responses of the interneuron to activation of a specific mechanosensory hair as identified by Letourneau (1976) on the tailfan should be compared among LDS interneurons having different patterns of dendritic branching. Further study is needed to determine if the morphological variability of the LDS interneuron leads to any functional variability or simply reflects the morphological differences in the pre- and post-synaptic cells.

Invariability in the LDS interneuron morphology

Physiological experiments have suggested that the dendrites on the side ipsilateral to the cell body function in receiving mechanosensory inputs while those on the contralateral side distribute these inputs to ascending interneurons (Krenz *et al.*, 1985; Reichert *et al.*, 1983). An electronmicroscopic study (Kondoh *et al.*, 1986) has demonstrated that ipsilateral dendrites are exclusively postsynaptic while contralateral ones have both input and output synapses intermingled on the same processes. In the present study, we have shown quantitatively for the first time that the dendritic structure is different between the ipsilateral and contralateral side at the light microscopic level. The ipsilateral dendrites are longer and more complex in branching pattern than the contralateral ones (Table 1). The difference in the whole dendritic length between both sides is mainly due to the difference in the length of fine dendrites (diameter < 6 μm). No significant difference is found in major dendrites (diameter > 6 μm). The spatial distribution of major dendrites was more stable among preparations than that of fine ones (Fig. 4).

The bilateral asymmetry in the dendritic structure of the LDS interneuron could be accounted for by different spatial distribution patterns of input and output cell processes. The interneuron has been reported to receive excitatory monosynaptic mechanosensory inputs from the uropod and telson on the ipsilateral side (Reichert *et al.*, 1983). These inputs originate from mechanosensory cuticular hairs and are carried to the terminal ganglion by sensory nerves entering from the first to 5th roots each having specific receptive field on the tailfan (Calabrese, 1976). The sensory nerve terminals are distributed so extensively in the ganglion (Kondoh *et al.*, 1987) that it is necessary for a cell to stretch out far-reaching dendrites in order to receive all of their inputs. The output target cells of the LDS interneuron have not been identified totally (Reichert *et al.*, 1983), but it is predictable from its bilaterally asymmetrical structure that the dendritic arborization of the target cells is more restricted than that of the LDS interneuron.

Another possibility is that the asymmetric structure might bestow some specific electrotonic characteristics on the interneuron which functions in conveying the ipsilateral synaptic input to the contralateral side. Apparently, the thinner and longer dendrites on the ipsilateral side are disadvantageous for effective spread of synaptic potentials than thicker and shorter dendrites on the contralateral side: potentials are attenuated more seriously and become slower in time course during their passive spread over the dendrite when the distance is longer and the space constant is shorter (Jack, 1979; Rall, 1977). However, the spatio-temporal distribution of synaptic potentials on dendrites is based on not only the anatomical properties of individual dendritic branches but also the three-dimensional branching pattern of the entire cell as well as the membrane properties of dendrites (Jack, 1979; Rall, 1977; Rall *et al.*, 1992). Therefore, comparison of anatomical parameters of individual branches alone is insufficient to understand the synaptic activity of a nerve cell. Functional significance of bilaterally asymmetrical dendritic structure of the LDS interneuron is still open to further analyses using its compartmental model based on three-dimensional dendritic structure and electrophysiological properties of the dendritic membrane (Perkel *et al.*, 1981; Segev *et al.*, 1989).

ACKNOWLEDGMENTS

This work was supported in part by Grants-in-Aid (Nos.07640894, 07554071) from Ministry of Education, Science, Sports and Culture of Japan.

REFERENCES

Borst A, Egelhaaf M (1994) Dendritic processing of synaptic information by sensory interneurons. Trends Neurosci 17: 257–263

Brodin L, Ericson M, Mossberg K, Hökfelt T, Ohta Y, Grillner S (1988) Three-dimensional reconstruction of transmitter-identified central neurons by "en bloc" immunofluorescence histochemistry and confocal scanning microscopy. Exp Brain Res 73: 441–446

Burrows M (1973) The morphology of an elevator and a depressor motoneuron of the hindwing of a locust. J Comp Physiol 83: 165–178

Burrows M, Siegler MVS (1976) Transmission without spikes between locust interneurones and motoneurones. Nature 262: 222–224

Calabrese R (1976) Crayfish mechanoreceptive interneurons. I. The nature of ipsilateral excitatory inputs. J Comp Physiol 105: 83–102

Carlson K, Wallén P, Brodin L (1989) Three-dimensional imaging of neurons by confocal fluorescence microscopy. J Microscopy 155: 15–26

Cullheim S, Fleshman JW, Glenn LL, Burke RE (1987) Membrane area and dendritic structure in type-identified triceps surae alpha-motoneurons. J Comp Neurol 255: 68–81

Fleshman JW, Segev I, Burke RE (1988) Electrotonic architecture of type-identified α-motoneurons in the cat spinal cord. J Neurophysiol 60: 60–85

Goodman CS (1978) Isogenic grasshoppers: Genetic variability in the morphology of identified neurons. J Comp Neurol 182: 681–706

Heitler WJ, Pearson KG (1980) Non-spiking interactions and local interneurons in the central pattern generator of the crayfish swimmeret system. Brain Res. 187: 206–211

Hisada M, Takahata M, Nagayama T (1984) Local non-spiking interneurons in the arthropod motor control systems: Characterization and their functional significance. Zool Sci 1: 681–700

Hoyle G (1975) Identified neurons and the future of neuroethology. J Exp Zool 194:51–74

Jack JJB (1979) An introduction to linear cable theory. In "The Neurosciences Fourth Study Program" Ed by Schmidt FO, Worden FG, MIT Press, Cambridge, MA, pp 423–438

Kondoh Y, Hisada M (1986) Regional specialization in synaptic input and output in an identified local nonspiking interneuron of the crayfish revealed by light and electron microscopy. J Comp Neurol 251: 334–348

Kondoh Y, Hisada M (1987) Neuroanatomy of the terminal (sixth abdominal) ganglion of the crayfish, *Procambarus clarkii* (Girard). Cell Tissue Res 243: 273–288

Krenz WD, Reichert H (1985) Lateralized inhibitory input to an identified nonspiking local interneuron in the crayfish mechanosensory system. J Comp Physiol 157: 499–507

Letourneau JG (1976) Addition of sensory structures and associated neurons to the crayfish telson during development. J Comp Physiol 110: 13–23

Macagno ER, Lopresti V, Levinthal C (1973) Structure and development of neuronal connections in isogenic organisms: Variations and similarities in the optic system of *Daphnia magna*. Proc Nat Acad Sci USA 70: 57–61

Mossberg K, Arvidsson U, Ulfhake B (1990) Computerized quantification of immunofluorescence-labeled axon terminals and analysis of co-localization of neurochemicals in axon terminals with a confocal scanning laser microscope. J Histochem Cytochem 38: 179–190

Nagayama T, Hisada M (1988) Bilateral local non-spiking interneurons in the terminal (sixth) abdominal ganglion of the crayfish, *Procambarus clarkii*. J Comp Physiol 163: 601–607

O'Shea M, Rowell CHF, Williams JLD (1974) The anatomy of a locust visual interneurone: The descending contralateral movement detector. J Exp Biol 60: 1–12

Pearson KG, Fourtner CR (1975) Non-spiking interneurons in walking system of the cockroach. J Neurophysiol 38: 33–52

Pearson KG, Goodman CS (1979) Correlation of variability in structure with variability in synaptic connections of an identified interneuron in locusts. J Comp Neurol 184: 141–166

Pearson KG, Heitler WJ, Steeves JD (1980) Triggering of locust jump by multimodal inhibitory interneurons. J Neurophysiol 43: 257–278

Perkel DH, Mulloney B, Budelli RW (1981) Quantitative methods for predicting neuronal behavior. Neurosci 6: 823–837

Rall W (1977) Core conductor theory and cable properties of neurons. In "Handbook of Physiology. The Nervous System. Cellular Biology of Neurons" sect 1, vol I, Ed by Kandel ER, American Physiological Society, Bethesda, Maryland, pp 39–97

Rall W (1981) Functional aspects of neuronal geometry. In "Neurones Without Impulses" Ed by Roberts A, Bush BMH, Cambridge University Press, Cambridge, pp 223–254

Rall W, Burke RE, Holmes WR, Jack JJB, Redman SJ, Segev I (1992) Matching dendritic neuron models to experimental data. Physiol Rev 72 (Supplement): 159–186

Reichert H, Plummer MR, Hagiwara G, Roth RL, Wine JJ (1982) Local interneurons in the terminal abdominal ganglion of the crayfish. J Comp Physiol 149: 145–162

Reichert H, Plummer MR, Wine JJ (1983) Identified nonspiking local interneurons mediate nonrecurrent, lateral inhibition of crayfish mechanosensory interneurons. J Comp Physiol 151: 261–276

Segev I, Fleshman JW, Burke RE (1989) Compartmental models of complex neurons. In "Methods in Neuronal Modeling" Ed by Koch C, Segev I, MIT Press, Cambridge, MA, pp 63–96

Sholl DA (1953) Dendritic organization in the neurons of visual and motor cortices of the cat. J Anat 87: 387–401

Shepherd GM, Koch C (1990) Dendritic electrotonus and synaptic integration. In "The Synaptic Organization of the Brain" (3rd edition) Ed by Shepherd GM, Oxford University Press, New York, pp 439–473

Spencer AN (1988) Non-spiking interneurones in the pedal ganglia of swimming mollusc. J Exp Biol 134: 443–450

Stewart, WW (1978) Functional connections between cells as revealed by dye-coupling with a highly fluorescent naphthalimide tracer. Cell 14: 741–759

Stretton AOW, Kravitz EA (1973) Intracellular dye injection: The selection of Procion yellow and its application in preliminary studies of neuronal geometry of the lobster nervous system. In "Intracellular Staining in Neurobiology" Ed by Kater SB, Nicholson C, Springer Verlag, New York, pp 21–40

Takahashi M, Takahata M (1995) Dendritic properties of uropod motoneurons and premotor nonspiking interneurons in the crayfish *Procambarus clarkii* Girard. J Comp Physiol 176: 503–512

Takahashi M, Takashima A, Takahata M (1995) Regional characteristics of the membrane response of an identified crayfish nonspiking interneuron to intracellularly injected current. J Neurophysiol 74: 2242-2250

Takahata M, Nagayama T, Hisada M (1981) Physiological and morphological characterization of anaxonic non-spiking interneurons in the crayfish motor control system. Brain Res 226: 309-314

Takahata M, Niwa M, Nakamura H (1995) Physiological characteristics

of the synaptic response of an identified sensory nonspiking interneuron in the crayfish *Procambarus clarkii* Girard. J Comp Physiol 176: 737–746

Treistman SN, Schwartz JH (1976) Functional constancy in *Aplysia* nervous systems with anomalously duplicated identified neurons. Brain Res 109: 607–614

Tweedle CD, Pitman RM, Cohen MJ (1973) Dendritic stability of insect central neurons subjected to axotomy and de-afferentation. Brain Res 60: 471–476

Ulfhake B, Kellerth J-OA (1981) A quantitative light microscopic study of the dendrites of cat spinal α-motoneurons after intracellular staining with horseradish peroxidase. J Comp Neurol 202: 571–584

Van Harreveld A (1936) A physiological solution for fresh water crustaceans. Proc Soc Exp Biol Med 34: 428–432

Wallén P, Carlsson K, Liljeborg A, Grillner S (1988) Three-dimensional reconstruction of neurons in the lamprey spinal cord in whole-mount, using a confocal laser scanning microscope. J Neurosci Methods 24: 91–100

Wilson T, Sheppard CJR (1984) Theory and Practice of Scanning Optical Microscopy. Academic Press, London

Wilson WA, Goldner MM (1975) Voltage clamping with a single microelectrode. J Neurobiol 6: 411–422